

An Analytic Model of Superclusters

Masamune Oguri†‡, Keitaro Takahashi‡, Kiyotomo Ichiki§||
and Hiroshi Ohno¶

†Princeton University Observatory, Peyton Hall, Princeton, NJ 08544, USA.

‡Department of Physics, University of Tokyo, Hongo 7-3-1, Bunkyo-ku, Tokyo 113-0033, Japan

§Division of Theoretical Astrophysics, National Astronomical Observatory, 2-21-1 Osawa, Mitaka, Tokyo 181-8588, Japan

|| Department of Astronomy, University of Tokyo, Hongo 7-3-1, Bunkyo-ku, Tokyo 113-0033, Japan

¶Institute for Cosmic Ray Research, University of Tokyo, 5-1-5 Kashiwa, Kashiwa City, Chiba 277-8582, Japan

Abstract. We construct an analytic model for the mass distributions of superclusters and clusters in each supercluster. Our model is a modification of the Press-Schechter theory, and defines superclusters as the regions that have some overdensity smaller than those for usual virialized objects. We compare the mass functions with a catalog of superclusters in the Sloan Digital Sky Survey Early Data Release and found that they are in reasonable agreement with each other.

1. Introduction

It is now known that our universe is hierarchical. The largest virialized objects in the universe are clusters that are made of hundreds of galaxies. Clusters have extensively been used to test structure formation models in the universe, through their abundances and correlations[1, 2].

Superclusters are defined as an ensemble of clusters. They are still assembling, and are even larger structure than clusters; superclusters have extents of $\sim 100\text{Mpc}$ or even larger. Thus superclusters offer us information on late evolution of universe, and also on the transition from linear to non-linear regime. Examples of the superclusters include A901/902[3], MS0302+17[4, 5], Cl1604+43[6, 7], the Sculptor supercluster[8], and the Shapley supercluster[9]. Detailed investigations have shown that these superclusters are real physical systems where clusters are gravitationally assembling. Detailed studies of these superclusters from galaxy distributions and weak lensing also showed that the mass distribution of superclusters is in good agreement with the distribution of early-type galaxies in superclusters. The physical state of gas in superclusters is still unknown, but it is worth mentioning that soft X-ray has been detected in the Sculptor supercluster[10].

Although most the studies have been limited to those of individual superclusters so far, the emergence of wide-field surveys/telescopes, such as the Sloan Digital Sky Survey (SDSS) and the Subaru Suprime-cam, begins to make it possible to do *statistical* studies of superclusters. Nevertheless, there is no analytic model of superclusters that predicts, e.g., the mass distribution. In this paper, we construct such an analytic model of superclusters. Basically, our model is a modification of the Press-Schechter theory[11], and predicts not only mass distributions of superclusters but also number distribution of clusters in each supercluster. We also compare our model with superclusters in the SDSS extracted by Einasto *et al.*[12]. Throughout the paper we assume a flat universe $\Omega_M + \Omega_\Lambda = 1$, and the Hubble constant $h \equiv H_0/(100\text{km s}^{-1}\text{Mpc}^{-1}) = 0.7$.

2. An Analytic Model

In this section, we construct the mass function of superclusters and clusters in each supercluster using the spherical model[11]. We regard superclusters as overdense regions that are on the course of the spherical collapse. Then superclusters can be defined as the regions that have the overdensity $\Delta_{\text{sc}} \equiv \rho_{\text{sc}}/\bar{\rho}$, where ρ_{sc} is the average density within superclusters and $\bar{\rho}$ is the mean density in the universe. Although superclusters are usually characterized by filamentary structure that is quite different from simple spherical overdensity, we consider this model so as to be analytically tractable. The assumption, however, may not be so crude given the similar situation that the Press-Schechter theory has achieved reasonable success despite its simplicity.

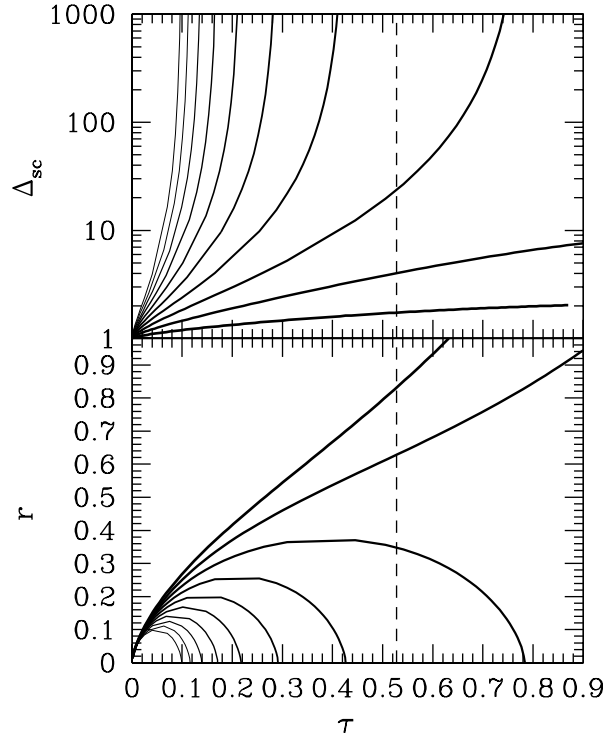


Figure 1. Sizes of overdense regions (r) and corresponding nonlinear overdensities (Δ_{sc}) as a function of dimensionless cosmic time τ . Different lines mean different values of κ : from $\kappa = 1$ (*Dark*) to 10 (*Light*). The vertical dashed line indicates the value of τ corresponding to $a = 1$. In this plot, we adopt $\Omega_M = 0.3$.

2.1. Spherical Model in Lambda-dominated Universes

Consider a spherical overdensity with mass M and radius R . Equation of motion of the overdensity is simply given by

$$\frac{d^2 R}{dt^2} = -\frac{GM}{R^2} + \Omega_\Lambda H_0^2 R. \quad (1)$$

By integrating this equation, we obtain

$$-E = \frac{1}{2} \left(\frac{dR}{dt} \right)^2 - \frac{GM}{R} - \frac{1}{2} \Omega_\Lambda H_0^2 R^2, \quad (2)$$

here $E > 0$ for a growing perturbation. We define

$$r \equiv \frac{R}{R_0}, \quad (3)$$

$$R_0 \equiv \left(\frac{2GM}{H_0^2 \Omega_M} \right)^{1/3}, \quad (4)$$

$$\kappa \equiv \frac{2E}{H_0^2 \Omega_M R_0^2}, \quad (5)$$

$$\tau \equiv \sqrt{\Omega_M H_0} t, \quad (6)$$

$$\omega \equiv \frac{1}{\Omega_M} - 1. \quad (7)$$

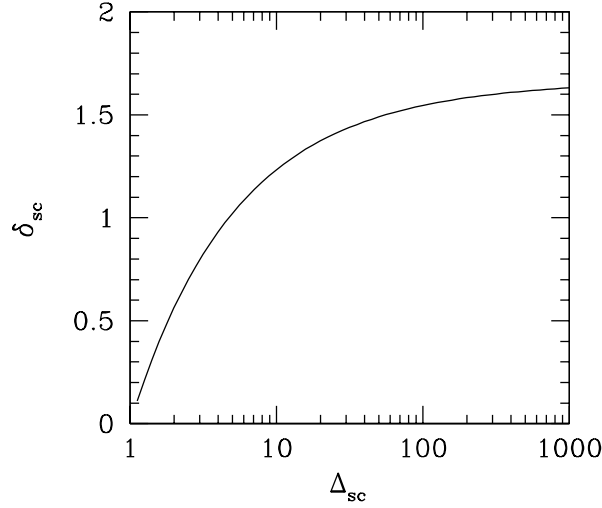


Figure 2. The relation of linear (eq. [10]) and nonlinear (eq. [11]) overdensities at $a = 1$. Here we adopt $\Omega_M = 0.3$.

Then equation (2) reduces to

$$\left(\frac{dr}{d\tau}\right)^2 = \frac{1}{r} - \kappa + \omega r^2. \quad (8)$$

On the other hand, the cosmological time is related with the scale factor as

$$\tau = \frac{1}{3}\omega^{-1/2}\text{arccosh}\left(1 + 2\omega a^3\right). \quad (9)$$

From equation (8), we can derive the motion of spherical overdensity as a function of τ . Figure 1 shows the evolution of the size of overdense region for various values of κ . It is shown that the corresponding overdensity Δ_{sc} increases monotonically as time evolves. Since the dimensionless time τ is related with the scale factor a as equation (9), at fixed time a and for fixed Δ_{sc} we can determine the value of κ uniquely by solving equations (8) and (9). Then the linear and nonlinear overdensity is easily derived:

$$\delta_{sc} = \frac{3\kappa}{5}D(a), \quad (10)$$

$$\Delta_{sc} = \frac{a^3}{R^3}, \quad (11)$$

where $D(a)$ is the linear growth rate normalized so that $D(a) = a$ at $a \ll 1$. From this, arbitrary Δ_{sc} is converted to the corresponding linear overdensity δ_{sc} that is an essential quantity in computing the mass function. In Figure 2, we plot an example of this relationship. It shows one-to-one correspondence between Δ_{sc} and δ_{sc} .

2.2. Mass Function of Superclusters and Clusters

To compute the mass function of superclusters, we adopt the Press-Schechter formalism[11]. From the linear overdensity δ_{sc} (eq. [10]), the mass function can be

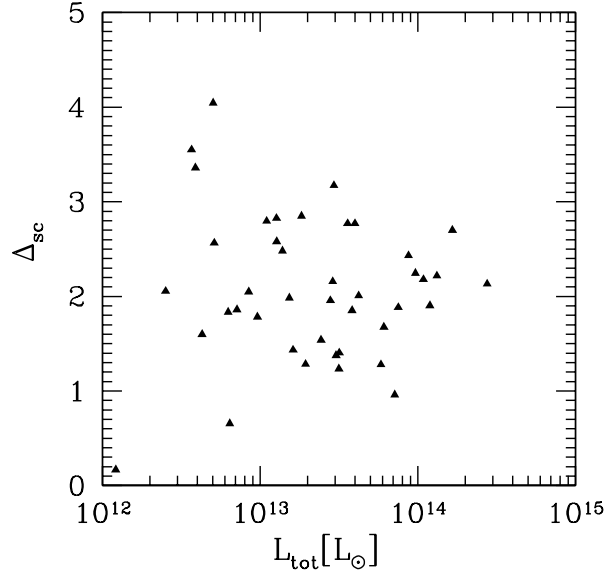


Figure 3. Overdensities versus total luminosities of superclusters in the SDSS EDR[12]. We assumed the average r -band luminosity density $\bar{\rho}_L = 2.6 \times 10^8 h L_\odot \text{Mpc}^{-3}$ [18] to convert into Δ_{sc} .

computed as

$$\frac{dn_{\text{sc}}}{dM} = \sqrt{\frac{2}{\pi}} \frac{\rho_0}{M} \frac{\delta_{\text{sc}}(z)}{\sigma_M^2} \left| \frac{d\sigma_M}{dM} \right| \exp \left(-\frac{\delta_{\text{sc}}^2(z)}{2\sigma_M^2} \right), \quad (12)$$

where $\delta_{\text{sc}}(z) \equiv \delta_{\text{sc}}\{D(z=0)/D(z)\}$, and σ_M is the (linear) mass variance at $z=0$.

The conditional mass function of clusters within superclusters, that are already virialized, can be estimated in analog with the extended Press-Schechter formalism[13, 14, 15]. The number of clusters with mass M that are in a supercluster with mass M_{sc} is given by

$$\frac{dn}{dM}(M|M_{\text{sc}}; z) = \frac{1}{\sqrt{2\pi}} \frac{M_{\text{sc}}}{M} \frac{\delta_c(z) - \delta_{\text{sc}}(z)}{(\sigma_M^2 - \sigma_{M_{\text{sc}}}^2)^{3/2}} \left| \frac{d\sigma_M^2}{dM} \right| \exp \left[-\frac{(\delta_c(z) - \delta_{\text{sc}}(z))^2}{2(\sigma_M^2 - \sigma_{M_{\text{sc}}}^2)} \right], \quad (13)$$

where $\delta_c(z) \approx 1.68\{D(z=0)/D(z)\}$ is the critical overdensity in the standard Press-Schechter formalism. Although the distribution of clusters in each supercluster might be affected by physical processes such as global tides and dynamical frictions[16], we adopt this form for simplicity.

3. Comparison with Observations

In this section, we compare our analytic model with the results of Einasto *et al.*[12] who made a catalog of superclusters in the SDSS Early Data Release (EDR)[17]. They extracted superclusters from the density field of galaxies with a smoothing length $10h^{-1}\text{Mpc}$, and also clusters from the density field with a smoothing length $0.8h^{-1}\text{Mpc}$. The superclusters and clusters are defined as the regions divided by the threshold density

($\delta = 1.8$). Since the SDSS EDR data consists of two slices, the density field is calculated in 2 dimensions only. Thus the total (r -band) luminosity of a supercluster is derived as

$$L_{\text{tot}} = \frac{D}{D_d} L_{\text{obs}}, \quad (14)$$

where D_d is the thickness of the slice, D is the average diameter of the supercluster, and L_{obs} is the observed luminosity with the selection function of galaxies corrected. With this way 39 superclusters were identified (see Table 3 of [12]).

Since the above definition of superclusters is slightly different from theoretical one, we need to check what the observed superclusters correspond to in our model. We have defined superclusters as the regions that have the overdensity Δ_{sc} , so we compute Δ_{sc} for each observed supercluster. Figure 3 shows Δ_{sc} for the SDSS EDR superclusters. Here we calculated Δ_{sc} as

$$\Delta_{\text{sc}} = \frac{L_{\text{tot}} / \{(4/3)\pi(D/2)^3\}}{\bar{\rho}_{\text{L}}}, \quad (15)$$

where $\bar{\rho}_{\text{L}} = 2.6 \times 10^8 h L_{\odot} \text{Mpc}^{-3}$ is the average r -band luminosity density[18]. This coincides with equation (11) if the mass-to-light ratio of superclusters is the same as that of the universe. As seen in the Figure, the derived value of Δ_{sc} is scattered at around 2 ($\Delta_{\text{sc}} = 2.1 \pm 0.8$). Thus we adopt $\Delta_{\text{sc}} = 2$ as a fiducial value, though we also examine the cases with $\Delta_{\text{sc}} \neq 2$ to see how the uncertainty of Δ_{sc} would affect our results.

3.1. Mass Function of Superclusters

First, we compare the abundance of superclusters in the SDSS EDR field. To do so, the volume of the field where superclusters were identified is needed. We simply adopt the sum of volumes of North and South slices of the EDR data[12]. However, this may underestimate the volume because of the correction outside the slices (eq. [14]). To convert mass functions of superclusters to luminosity functions, the mass-to-light ratio of superclusters. Again, we assume the fiducial model $M/L = 400hM_{\odot}/L_{\odot}$, and estimate the sensitivity by changing M/L from $250hM_{\odot}/L_{\odot}$ to $500hM_{\odot}/L_{\odot}$.

Figure 4 plots luminosity functions of superclusters in theory and observations. First, the abundance of massive superclusters is sensitive to Δ_{sc} , thus the selection of superclusters is quite important in comparing the abundance. Next, the abundance of massive superclusters is also very sensitive to σ_8 . Therefore, surveys of massive superclusters can be a good probe of σ_8 . Finally, the observed number of superclusters shows reasonable agreement with the theory, particularly when we take account of several uncertainties including that of the survey volume. At smaller luminosities the difference seems large, but this may be ascribed to the incompleteness of observations for such small objects.

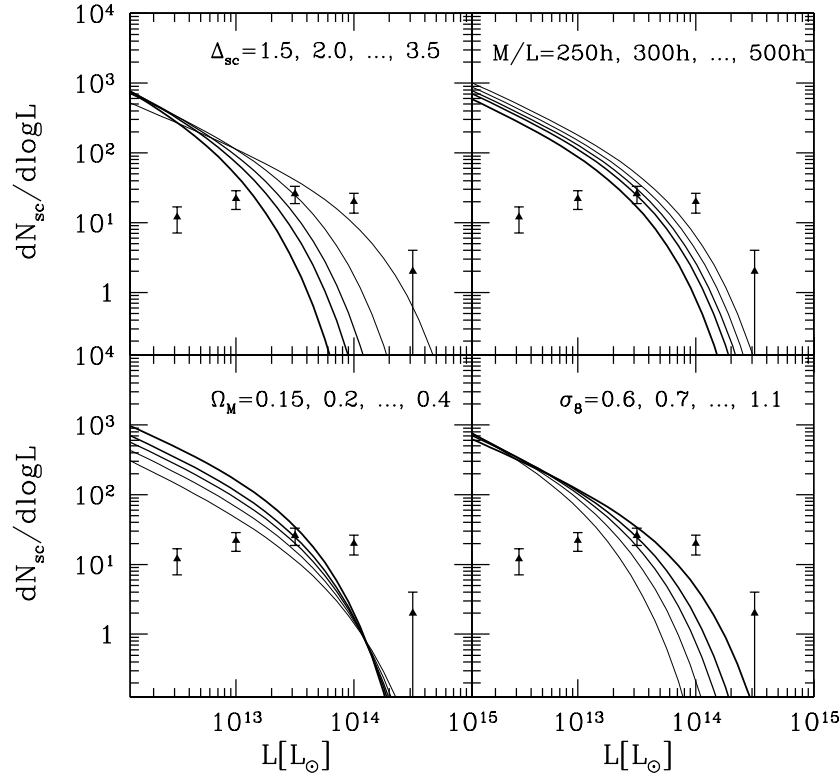


Figure 4. Comparison of luminosity functions of superclusters. The observational data (*filled triangles with errorbars*) are taken from [12]. For the errorbars, only statistical errors are included. We adopt the following fiducial model in computing theoretical predictions: $\Delta_{\text{sc}} = 2.0$, $M/L = 400hM_{\odot}/L_{\odot}$, $\Omega_M = 0.3$, and $\sigma_8 = 0.9$. For each panel, we changed one of these parameters while the other parameters are fixed. In all panels, the darker lines mean the larger values.

3.2. Number of Clusters in Superclusters

Einasto *et al.* also estimated the number of clusters in each supercluster. They noted that there exists a well-defined lower limit of cluster luminosities that is a function of distance to clusters (denoted by d), particularly for those at larger distances (see Figure 6 of [12]). Thus we divide the supercluster sample by the distance d . For each subsample, we assume the limiting luminosity shown in Figure 6 of [12] and calculate the number of clusters in a given supercluster by integrating equation (13). We also convert the observed number of clusters in the EDR field to the *total* number in the similar way as equation (14).

In Figure 5, we plot the number of clusters within superclusters for different distances d . We find that theoretical curves and observations show good agreement with each other. It seems that the model overpredicts the number of clusters, but this is perhaps because the assumption of the existence of lower limit of cluster luminosities becomes inaccurate for lower d (see Figure 6 of [12]). Next we examine the dependence of several parameters on the number of clusters, which is shown in Figure 6. The

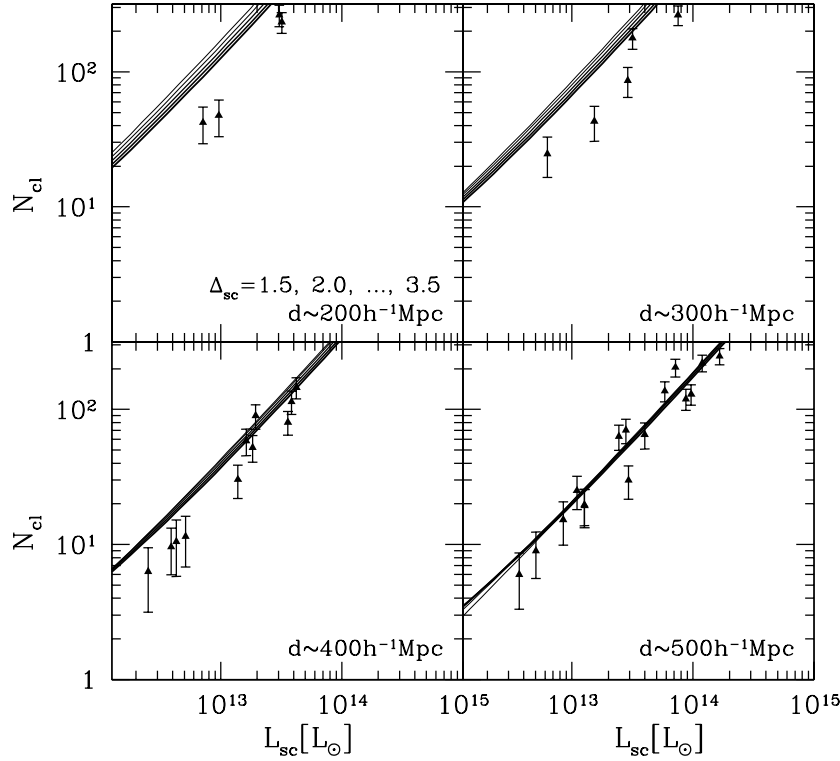


Figure 5. Comparison of the numbers of clusters in superclusters. The observational data (*filled triangles*) are taken from [12]. For the errorbars, only statistical errors are included. We consider four subsamples of superclusters divided by the distances to superclusters; $d \sim 200h^{-1}\text{Mpc}$ ($150h^{-1}\text{Mpc} < d < 250h^{-1}\text{Mpc}$; *upper left*), $d \sim 300h^{-1}\text{Mpc}$ ($250h^{-1}\text{Mpc} < d < 350h^{-1}\text{Mpc}$; *upper right*), $d \sim 400h^{-1}\text{Mpc}$ ($350h^{-1}\text{Mpc} < d < 450h^{-1}\text{Mpc}$; *lower left*), and $d \sim 500h^{-1}\text{Mpc}$ ($450h^{-1}\text{Mpc} < d < 550h^{-1}\text{Mpc}$; *lower right*). As limiting masses of clusters, we adopt “set 1” in Figure 6 of [12]. Different lines mean different values of Δ_{sc} . The other parameters are fixed to the fiducial values (see the caption of Figure 4).

Figure indicates that the number of clusters in superclusters hardly depends on these parameters, though that was already clear from the expression of the conditional mass function shown in equation (13). Thus the model predictions are quite robust, and the good agreement means that our model works well.

4. Summary and Discussion

In this paper, we have constructed an analytic model of superclusters. Our model is based on the Press-Schechter theory, and defines superclusters as overdense regions that are on the course of the spherical collapse. Our model allows us to compute the mass function of superclusters, and also the number distributions of clusters in each supercluster.

To test the model, we have compared the model with the supercluster catalog in the SDSS EDR data. We have shown that the model shows in reasonable agreement with

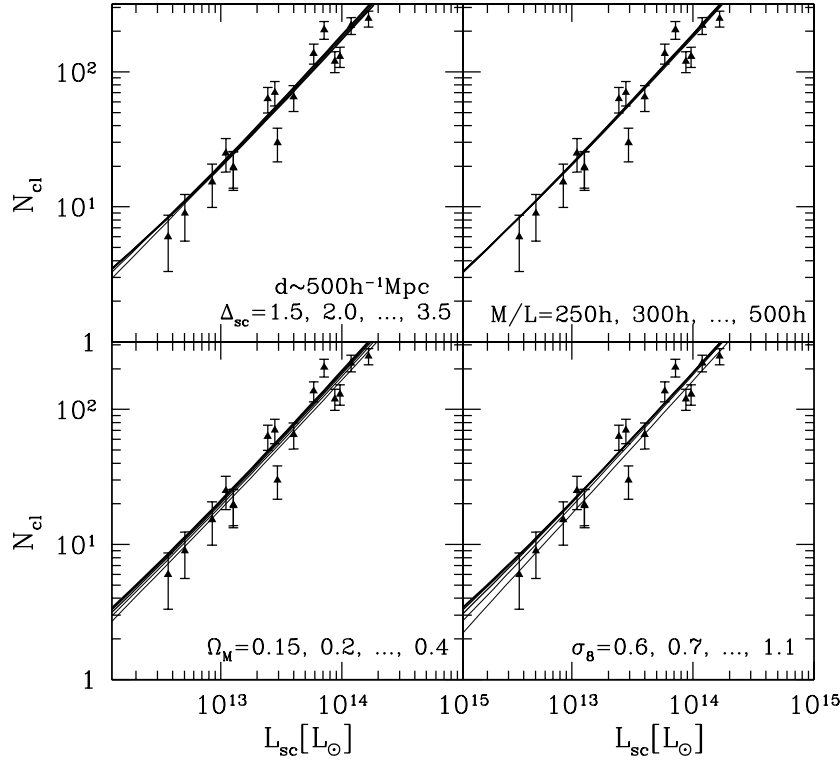


Figure 6. Comparison of the numbers of clusters in superclusters at $d \sim 500h^{-1}\text{Mpc}$. The observational data (*filled triangles*) are taken from [12]. For the errorbars, only statistical errors are included. For each panel, we changed one parameters while the other parameters are fixed to the fiducial values (see the caption of Figure 4). In all panels, the darker lines mean the larger values.

the observation. We have also examined parameter dependences of the mass function of superclusters, and found that the mass function of massive superclusters is sensitive to σ_8 . Thus superclusters will be a useful probe of σ_8 if superclusters are selected more rigorously. On the other hand, the number of clusters in superclusters shows only weak dependences on parameters.

Our model would be useful not only in constraining cosmological parameters from the abundance of superclusters but also in many applications. One of such applications is hot gas in superclusters. Recently it has been claimed that soft X-ray[10] and Sunyaev-Zel'dovich effects[19] in the supercluster regions may be detected, and this might suggest the existence of relatively hot gas in superclusters. If this is true, the statistical significance of the signals that are caused by the hot gas can be computed by using our model, once the we measure the temperature and density structure of hot gas. Other application is gravitational lensing; gravitational lensing measures the total mass along the line of sight, thus a supercluster outside a cluster may affect, e.g., the mass estimate of the cluster. Our model is useful since it allows us to estimate the distribution of the host superclusters for a given cluster. In practice, we found that the effect is negligible when we consider superclusters with $\Delta_{\text{sc}} \sim 2$; assuming

a homogeneous sphere, convergence of a supercluster with $M = 10^{16}h^{-1}M_{\odot}$ can be estimated as

$$\kappa = \frac{\Sigma}{\Sigma_{\text{crit}}} \sim \frac{9 \times 10^{12} (M/10^{16}h^{-1}M_{\odot})^{1/3} (\Delta_{\text{sc}}/2)^{2/3} h M_{\odot} \text{Mpc}^{-2}}{4 \times 10^{15} h M_{\odot} \text{Mpc}^{-2}} \sim 2 \times 10^{-3}, \quad (16)$$

where we assumed a source at $z \sim 1$ and a supercluster at $z \sim 0.3$. However, it is of interest to consider the effect more carefully, because the effect is dependent on the density profile of superclusters as well as the definition of superclusters, Δ_{sc} . In particular, superclusters could have much more significant effect if superclusters have centrally concentrated density distributions.

Although our model looks successful at this moment, definitely we need more tests. The more direct way to test the model is to compare it with numerical simulations, since we know the initial condition and cosmological parameters in numerical simulations. Of course, comparison with observations is also of great importance in order to test our understanding of the universe. Now the SDSS data have been becoming public[20, 21], and the quite large survey region of the SDSS would allow us to make three-dimensional catalog of superclusters. The follow-up work is currently in progress, and the results will be presented elsewhere.

Acknowledgements

We thank Issha Kayo for useful discussions. MO, KT, and KI are supported by JSPS through JSPS Research Fellowship for Young Scientists.

References

- [1] N. A. Bahcall and R. M. Soneira, *Astrophys. J.* **270**, 20 (1983)
- [2] N. A. Bahcall and R. Cen, *Astrophys. J.* **398**, L81 (1992)
- [3] M. E. Gray, A. N. Taylor, K. Meisenheimer, S. Dye, C. Wolf and E. Thommes, *Astrophys. J.* **568**, 141 (2002)
- [4] D. G. Fabricant, M. W. Bautz and J. E. McClintock, *Astron. J.* **107**, 8 (1994)
- [5] R. Gavazzi, Y. Mellier, B. Fort, J.-C. Cuillandre and M. Dantel-Fort, *Astron. Astrophys.* **422**, 407 (2004)
- [6] L. M. Lubin, R. Brunner, M. R. Metzger, M. Postman and J. B. Oke, *Astrophys. J.* **531**, L5 (2000)
- [7] R. R. Gal and L. M. Lubin, *Astrophys. J.* **607**, L1 (2004)
- [8] P. Schuecker and H. Ott, *Astrophys. J.* **378**, L1 (1991)
- [9] H. Quintana, A. Ramirez, J. Melnick, S. Raychaudhury and E. Slezak, *Astron. J.* **110**, 463 (1995)
- [10] L. Zappacosta, R. Maiolino, F. Mannucci, R. Gilli and P. Schuecker, *Mon. Not. R. Astron. Soc.* submitted (astro-ph/0402575)
- [11] W. H. Press and P. Schechter, *Astrophys. J.* **187**, 425 (1974)
- [12] J. Einasto, G. Hütsi, M. Einasto, E. Saar, D. L. Tucker, V. Müller, P. Heinämäki and S. S. Allam, *Astron. Astrophys.* **405**, 425 (2003)
- [13] R. G. Bower, *Mon. Not. R. Astron. Soc.* **248**, 332 (1991)
- [14] J. R. Bond, S. Cole, G. Efsthathiou and N. Kaiser, *Astrophys. J.* **379**, 440 (1991)
- [15] C. Lacey and S. Cole, *Mon. Not. R. Astron. Soc.* **262**, 627 (1993)
- [16] M. Oguri and J. Lee, *Mon. Not. R. Astron. Soc.* in press (astro-ph/0401628)
- [17] C. Stoughton *et al.*, *Astron. J.* **123**, 485 (2002)

- [18] M. R. Blanton *et al.*, Astron. J. **121**, 2358 (2001)
- [19] A. D. Myers, T. Shanks, P. J. Outram, W. J. Frith, A. W. Wolfendale, Mon. Not. R. Astron. Soc. **347**, L67 (2004)
- [20] K. Abazajian *et al.*, Astron. J. **126**, 2081 (2003)
- [21] K. Abazajian *et al.*, Astron. J. **128**, 502 (2004)